Digital Clay:
User Interaction Model for Control of a Fluidically Actuated Haptics Device

Stephen A. ASKINS, Wayne J. BOOK
Woodruff School of Mechanical Engineering
Georgia Institute of Technology
Atlanta, GA 30332
(stephen.askins@me.gatech.edu)
(wayne.book@me.gatech.edu)

ABSTRACT

Digital Clay is a novel haptics device the purpose which is to form a continuously variable surface that can be used to display shape data or accept shape input. It will be composed of a large number of small fluidic actuators and an array of MEMS micro-valves. Teams are investigating the kinematic architecture, the human interface, the control, the fluidics, and the valve design for this device. This paper describes the development of a computer model to simulate the device as well as human interaction with it via a simulated fingertip. The model is developed for a conceptual architecture design that could be used in a future prototype wherein the surface is defined by a close-packed array of slender fluidic actuators, however other architectures are also discussed. A key element of controlling this device will be interpreting user input. Therefore the simulations presented attempt to validate algorithms for tracking the user's finger and producing variable height bosses and creases in the surface.

Keywords: haptics, user interface, control, MEMS

NOMENCLATURE

A_a	Area of the actuator	f_{di}	Finger element distance coefficient
b_e, m_e	Coefficients of elastic response	$G(t)$	QLV Relaxation Function
c_i, v_i	Coefficients of relaxation function	$G'(t)$	Modified QLV relaxation function
c'_i, v'_i	" of modified relaxation function	Pa	Pressure in actuator
C_q	Valve discharge coefficient	q	Flow through valve into actuator
d_o	Valve orifice diameter	Q	Flow through valve
D_a	Diameter of actuator	r_{VM}	VM search space for Method I
h^*	Valve coefficient	$r_{blister}$	Blister radius (both methods)
h_v	Maximum valve stroke	R	Flow resistance factor
H	Height of the actuator	Re^*	Special Reynolds number
F_{aj}	Force applied on actuator j	$T^{(e)}$	QLV elastic function
F_{ei}	Force response of finger element i	ρ	Density of the fluid
F_{ref}	Set-point force for FF control	τ_v	Valve time constant
F_{trig}	Triggering force for state transition	v	Kinematic viscosity

1 INTRODUCTION

The power of modern personal computers brings engineers, designers, artists, and others the ability to represent complex three-dimensional shape data in a digital environment where it may be easily altered, analyzed, exported to other formats, and even used to create physical objects through rapid prototyping and computer aided manufacturing. However, with few exceptions, the means of interacting with the data are two-dimensional devices: the computer monitor and mouse.

The Digital Clay project at Georgia Tech [1] seeks to provide a much more intuitive means of interacting with virtual shapes in three dimensions. The goal of this project is to create a desktop-sized computer input/output device which presents the user with a surface that is continuously deformable either directly by the force of the user's hand, or under computer control. Digital Clay may be sculpted like real clay, but it also may be used to produce in real time physical models of three-dimensional shape data, portray the stiffness or softness of an object, or react intelligently to predict user intention from the forces applied.

Various architectures to accomplish these goals are being considered, however all include a very large number of relatively small fluidic actuators, or cells, that work in parallel to control the surface. The fluid flow to these actuators will be controlled via dedicated MEMS micro-valves. All aspects of its design should be fully scalable.

This article describes an initial model of a potential prototypical design of this device to evaluate high-level coordinated control schemes. In particular we attempt to anticipate issues related to controlling a large number of actuators and interpreting user input.

2 RELATED WORK

Currently haptic interaction with personal computers is limited to point contact with a virtual object displayed on a monitor. The commercially available PHANToM device [2] is a good example of this approach. Other related work includes tactile displays created using arrays of pins with a relatively low stroke, and often only binary operation, that are meant to recreate certain tactile sensations directly on the fingertip [3-5]. The Digital Clay project, on the other hand, proposes to provide an actuated, instrumented, physical volume to act as a haptic communication device. Project FEELEX, [6], has similar goals but a much smaller scope

3 DEVICE MODEL

The potential Digital Clay architecture explored here uses a closely packed array of slender fluidic cylinders to describe a surface as shown in Fig. 1.

Although the final digital clay design will possibly use a more advanced architecture, such as the proposed "formable crust" architecture [7], it is likely that an interim prototype of pin design will be produced since the technology for manufacturing these more complex architectures does not yet exist.
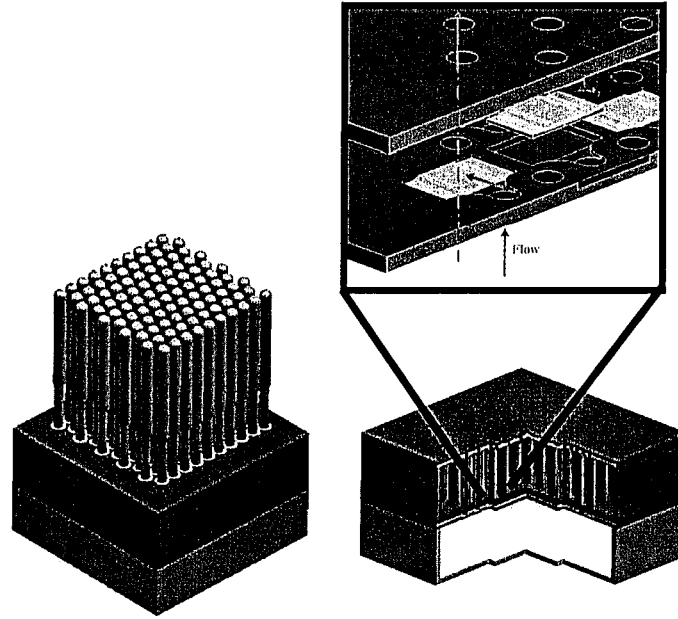
Figure 1: Potential Digital Clay architecture.

We have chosen to model an array of 625 actuators in either gridded (aligned) or staggered formation, with a nominal spacing of 3 mm. The figures in this paper, for clarity, portray a 10 by 10 configuration. A more detailed schematic appears in Fig. 2. The assumed actuators, which could be created using a rapid prototyping technique that is not the focus of this paper, are given an overall diameter of 2mm and a vertical stroke of 100 mm. These actuators are each supplied with low or high pressure fluid via piezoelectric, proportional, MEMS valves. The pressure reservoirs are stacked directly below the actuators to minimize the length of the fluidic conduits. There are two reservoirs, one maintained at 0.5 bar and the other at -0.5 bar relative to atmospheric pressure, used to raise and lower the cells respectively. The valves are created of-a-piece in flat arrays that form the top of the reservoirs. The upper reservoir includes conduits that pass fluid from the lower reservoir. The fluid is taken to be a low viscosity hydraulic fluid (e.g. silicone based).

The defining equations of the device model are intentionally simplified. Because we are not modeling an actual device, high numerical accuracy of the results is not important. Rather, we are interested in producing a representative behavior based on the following assumptions.

First, we assume the working fluid is completely incompressible. Therefore, that the resulting height is a direct integral of the fluid flow. Additionally, we assume quasi-static fluid state. That is, the pressure in the actuator is related only to the applied force on the cell and not the flow into and out of it.

$$H = \int_0^t q \cdot d\tau \Big/ A_a \quad ; \qquad P_a = \frac{F_a}{A_a} \qquad\qquad (1,2)$$
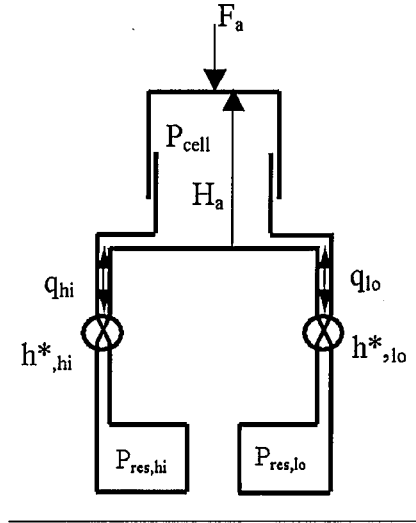
Figure 2: Basic cell diagram.

The valves to be used are currently under development by the MEMS group of the Digital Clay team, and therefore not available for experimental characterization. Analytical models for macro-sized valves are not applicable to valves on this small scale. However Carretero and Breuer have published data for a 10:1 scale model of a similarly configured micro-valve [8], and we were able to adapt this information to build an approximate empirical valve model. They publish discharge coefficients vs. a specially defined Reynolds number for a variety of fractional valve openings, h*.

$$C_q = \frac{4 \cdot Q}{\pi \cdot d_o} \cdot \sqrt{\frac{\rho}{2\Delta P}} \; ; \quad \mathrm{Re}* = \sqrt{\frac{Q}{v \cdot h_v}}$$

(3,4)

Their data can be simplified by the following model:

$$C_q = \begin{cases} 0.18 h^* & if\ \mathrm{Re}^* \geq 200 \\ \dfrac{0.18 h^* \cdot \mathrm{Re}^*}{200} & if\ \mathrm{Re}^* < 200 \end{cases}$$

(5)

And then equations (3-5) can be used to derive an expression for volumetric flow as a function of pressure drop across the valve as follows:

$$\Delta P^{crit} = \frac{3.9 \times 10^{11} \cdot \rho \cdot h^{*2} \cdot v^4 \cdot h_p^{\ 4}}{\pi^2 \cdot d_o^4}$$

(6)

$$Q = \begin{cases} \dfrac{\pi \cdot h * \cdot d_o^2}{22.2} \sqrt{\dfrac{2\Delta P}{\rho}} & \text{if } \Delta P \geq \Delta P^{crit} \\[3mm] \dfrac{\pi^2 \Delta P \cdot h * \cdot d_o^4}{9.9 \times 10^6 \cdot v \cdot h_p \cdot \rho} & \text{if } \Delta P < \Delta P^{crit} \end{cases}$$

(7)

Equation (7) represents fully developed laminar flow in the valve only. To account for the pressure loss in the conduits the Hagen-Pouiselle law is employed.

$$\Delta P_c = \frac{Q \cdot 128 \cdot L_c \cdot \mu}{\pi \cdot D_c^4}$$

(8)

Also, there are sure to be transient effects when the valve position is opened, closed, or changed. There will also be some response time required to physically open the valve. These transient effects are lumped together as a single first order response of time constant, τ_v, and a direct time delay, t_d:

$$\tau_v \dot{K}_v(t) + K_v(t) = K_{v,com}(t - t_d)$$

(9)

5 FINGER MODEL

The finger model is based on the Fung's quasi-linear viscoelastic (QLV) model for human tissue. [9] This model describes the stress relaxation of tissue over time. Specifically, parameters used in this paper were taken from the work of Pawluck in characterizing the human fingertip. In her work [10, 11], she characterized the force response of the center of the fingerpad of a number of subjects to a single indenter. Her application of the QVC model can be defined as:

$$F_{e,i}(t) = T^{(e)} \cdot [x(t)] + \int_0^t T^{(e)} \cdot [x(t-\tau)] \frac{\partial G(\tau)}{\partial \tau} d\tau$$

(10)

where the force response of the finger is a combination of the elastic response $T^{(e)}$ which is the instantaneous response of the finger and some relaxation function $G(t)$. Pawluk found that the elastic function is approximated by an exponential spring:

$$T^{(e)}(x) = \frac{b_e}{m_e} \left[e^{m_e(x-x_0)-1} \right]$$

(11)

and the relaxation can be approximated by a superposition of three time constants.

$$G(t) = \left(c_0 + \sum_{i=1}^{3} c_i e^{-v_i t} \right) \bigg/ \sum_{i=1}^{3} c_i$$

(12)

The parameters in equations (11-12) are found experimentally by Pawluk using a number of subjects.

It has been found that the convolution of (10) makes the system more difficult to simulate. However modeling the relaxation as three separate, parallel first order systems as follows can accurately approximate the response:

$$G_i^*(t) = c_0^* v_i \int T^{(e)}(\delta(t)) dt \tag{13}$$

$$F_e^*(t) = T^{(e)}(\delta(t)) \cdot \left[1 - \sum_{i=1}^{3} (c_i^* \cdot G_i^*(t)) \right] \tag{14}$$

where the c_i^* are calculated to give the same response as (10).

This model was verified based on data found by Gulati [12] and others. To incorporate the spatial extent of the finger-tip, a finger "element" that follows the laws of the equations is added to each actuator. This element is only "active" when the finger is determined to be above that actuator. Furthermore the undeformed height used is found by assigning the fingertip an elliptical shape.

6 CONTROL METHODS

A fully realized digital clay device might include three levels of control. The top level, existing as software on the interfaced PC, produces a commanded shape, or possibly a commanded pressure field. The second level of control would transform that desired shape into individual actuator commands, using inverse kinematics if necessary. Finally, the lowest level of control would feedback sensor information and open and close valves such that the correct actuator state (either size or pressure level) is attained.

For a detailed study of single-actuator control of digital clay, please see a related paper by Haihong Zhu of the Digital Clay team [13]. The object of this paper, though, is to study methods for the concerted control of all the actuators of the modeled device in order to produce a specified goal. Specifically our goal is to implement a shaping method developed by the User Interface group, which has been termed "blister tracking." [14]

In this interaction scheme, the finger is tracked using a controlled local deformation in the Clay's surface. Once this local deformation has been activated, force-control is used to maintain contact with the finger. As the finger moves, the local deformation, or "blister" follows it. If the surface is commanded to maintain its shape after being deformed by the blister, a boss or crease will be formed on the existing surface along the trajectory that the user traces with his finger.

This scheme is an ideal test-bed for early investigations because it limits the simulation of human interaction to one fingertip only. Also, it poses a complex coordinated control problem, that may be a good measure of Digital Clay's capacity. It also may be an ideal method of shape editing to adding fine features to the Digital Clay Surface.

7 FINGER TRACKING METHODS

Two primary methods for implementing this finger tracking technique have been chosen and tested. The first is a high-level control technique that bases actuator height commands on a single virtual actuator. The second method combines intelligence at the actuator level to produce coordinated blister creation.

In the first method, an imaginary actuator is placed directly beneath the finger at all times. All of real actuators are slaved to this Virtual Master actuator (VM). The profile by which the commanded heights are produced from the VM height describes the blister. Control is accomplished by four modules: *VM Locate*, *VM Control*, *VM Model*, and *Blister Creation*, related as shown in Fig. 3.
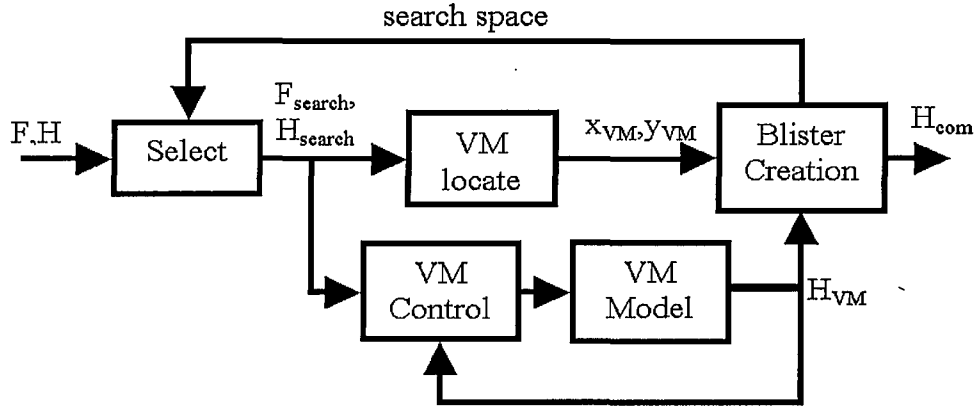
Figure 3: Blister Tracking Controller Method I Block Diagram

The *VM Locate* module's purpose is to constantly provide a current location to the blister creation module. This location is defined to be the centroid of the current applied force on all cells in a certain search area, defined as those cells within a certain radius, r_{VM}, from the former VM position. When the finger has just touched the device, there is no previous VM position, and the entire surface is searched. Using a subset of the cylinders to search for the VM speeds the calculation and prevents force noise from affecting the calculation. Currently r_{VM} is equal to the average radius of a human finger though this size could be optimized depending on controller sampling rate.

$$\bar{r}_{VM} = \frac{\sum_{j=f_1}^{f_n} F_j^a \cdot \bar{r}_j}{\sum_{j=f_1}^{f_n} \bar{r}_j} \tag{13}$$

where $j = [f_1 \cdots f_n]$ represent actuators, j, such that $\left| \bar{r}_j - \bar{r}_{VM, former} \right| \le \left| r_{VM} \right|$.

The *VM Control* module controls the current height of the virtual master. Control effort is equivalent to the valve coefficient of an actual cylinder. The *VM Model* module is essentially a model of a physical cylinder that converts this valve coefficient into a cylinder height.

In the current implementation, *VM control* has two modes, similar to the mode of single actuator control used in [13], although a plastic response mode is not used. Initially the master is controlled to respond as a virtual spring. In other words the commanded height at any given time is calculated from the perceived total force using an inverse spring law. The force is the total force in the VM search area, which corresponds to the area under the finger. Once this force reaches a certain force F_{trig}, the controller enters shaping mode. In this mode the virtual master attempts to "stick" to the finger. VM height is adjusted, using force control, to maintain a set-point force F_{ref}. This causes it to follow the finger.

Finally, *Blister Creation* accepts the VM position and height and uses a blister profile to generate height commands for all actuators. Only commands for actuators within a certain radius, $r_{blister}$, of the VM are altered, but earlier commands are maintained once the actuator ceases to be in the area of influence. Though the actual profile of the blister is variable, experiments so far have used a linear, flat-topped cone, and a Gaussian curve. Profiles are described via radial coordinates, where the VM position is the origin, and as a proportion of the height difference between the VM height and the height at the edge. To determine profile edge height, the heights of actuators just outside the blister are used. Fig. 4 illustrates the blister and edge concepts in 2D.
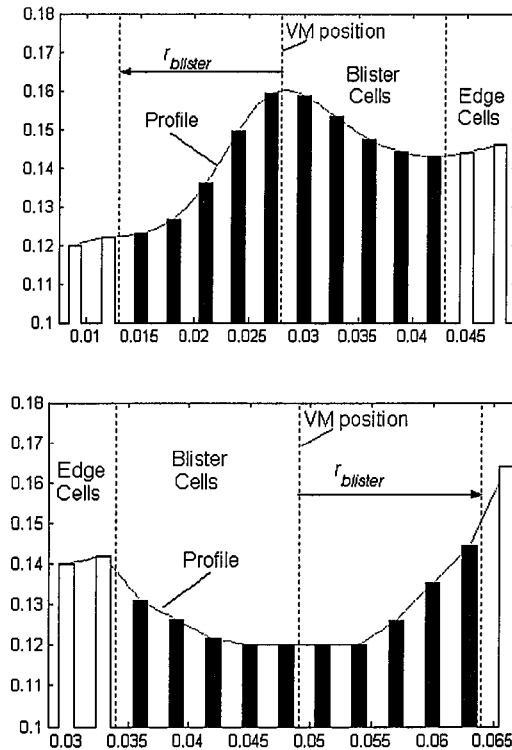
Figure 4: Sample 2D convex and concave blisters

The height commands are then sent to the actuator controller, which in this implementation is simple proportional control.

In the second method, the actuators all possess a current control state of virtual spring (*VS*), follow finger (*FF*), or blister. Fig. 5 shows the state transition diagram for a given cell. The *VS* and *FF* modes are similar to the modes of the VM controller described above, though applied to a single actuator. All actuators are initialized to *VS* mode. Once F_{trig}^{VS} is reached, a transition to the *FF* set force controller occurs. Also, during this transition, all cells within a radius $r_{blister}$ are simultaneously set to blister mode. These cells are then commanded to form a blister profile that blends the heights of the *FF* cells with those of the *VS* cells. The blister controller is similar to the blister module from method I, with the correct modifications given
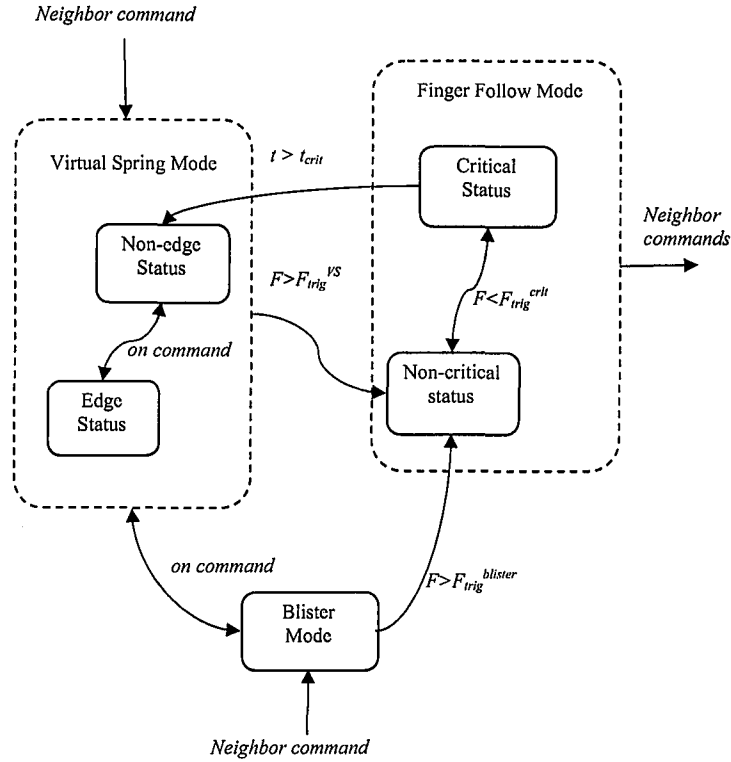
Figure 5: State transition diagram, Method II.

that there is not one single master but a group of cells under *FF* control that serve to define the blister height and location.

Cells that are in blister mode also transition to *FF* when their force is greater than $F_{trig}^{blister} < F_{trig}^{VS}$.

The intention is that this force is low enough that virtually any finger contact will trigger the transition. Therefore when a single actuator transitions to *FF* mode and sets its neighbors to blister mode, any of those neighbors who are currently contacting the finger will also immediately transition to *FF* mode, extending the blister. All actuators directly under the finger are rapidly located without a coordinating intelligence.

This effect also accomplishes the task of tracking the finger. By incorporating a slight rise in the blister profile we can ensure that the actuators will feel additional force if the finger is moved in any direction, and therefore transition to state *FF*.

FF cells whose applied force falls below a certain amount are labeled *critical*. They will transition back to *FF* if their sensed force rises back above F_{trig}^{crit}, if they remain critical for a certain amount of time they instead transition to *blister* state.

Every time an actuator transitions to or from *FF* mode, a routine to redefine the blister cells is called and the new set of cells in *FF* mode is used. This ensures that the actuators following blister control are always the superposition of the neighbors of every current *FF* cell, except for those actuators that are themselves under finger follow control. Also, in this routine one more actuator state, *edge*, is defined for those cells that are a distance $r_{blister} \le r < r_{edge}$ from

the *FF* cell in question. The heights of these cells are used as in Method I to find the heights at the blister boundary for the profile calculation. These actuators follow the *VS* control law.

However the aim is not only to create a blister that moves with the finger, but also to cause this blister to leave behind it a ridge or trench that shares its cross section. Therefore, an additional aspect to both methods is the concept of "freezing" the actuators when the blister is in motion, so that the desired final surface is achieved. Although implemented slightly differently for these two methods, they both are given the ability to detect which actuators are being moved away from, and command those actuators to maintain the commanded height until they are no longer in the blisters area of influence, as illustrated by Fig. 6.

In the simulation these state transitions are accomplished with vector manipulation for efficiency but they could be implemented in a physical model with inter-cell communication.
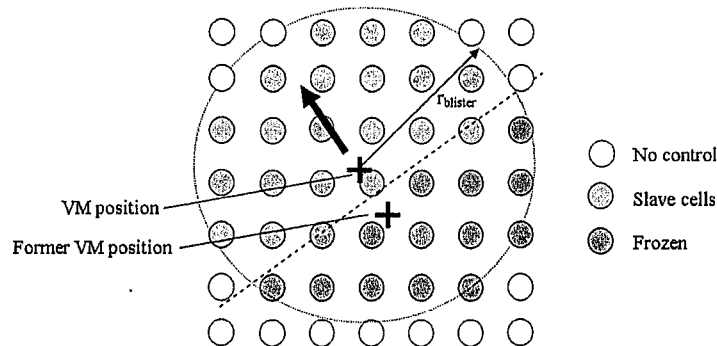

Figure 6: Freezing to create bosses and creases

8   RESULTS AND DISCUSSION

A visual tool (Fig. 7), is used that creates animations of the actuator movement and simultaneously displays forces and actuator control modes. Without such an animation communicating the overall behavior of the device is difficult.

Early simulations focused on validating the various components of the model, as well as the marriage of the finger model with the device model. Later, the control methods outlined in
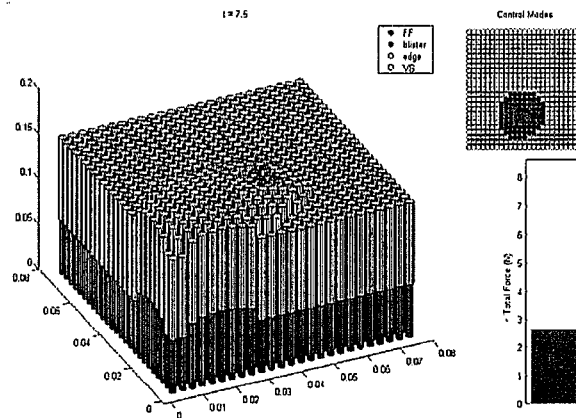

Figure 7: Visualization tool

Section 7 were implemented and various finger trajectories were used as inputs to test both the concept and the implementations of the methods. Performance is highly dependent on control parameters used. However both methods were able to maintain blister tracking on reasonably simple trajectories for horizontal finger speeds up to 15 mm/sec.

We present here results from a representative trajectory wherein the finger first pushes into the surface near the corner viewed as in Fig. 8 and Fig.9, initializes a blister, and "lifts" it to a height such that the blister is about a centimeter and a half over the initial surface. Then the finger drags the blister, levelly, to a point near the other edge of the device and rises up slowly to create a "mound" above the end of the "ridge". Then the finger is quickly removed. A second later the finger returns and pushes into the surface at the far-left corner. This time it stays below the surface, and creates a "valley" across the far edge of the surface.

In Fig. 8 the height trajectories (a,c) of selected actuators are shown along with total forces felt by the simulated finger (b,d) for both methods. Fig. 10 shows the resulting actuator
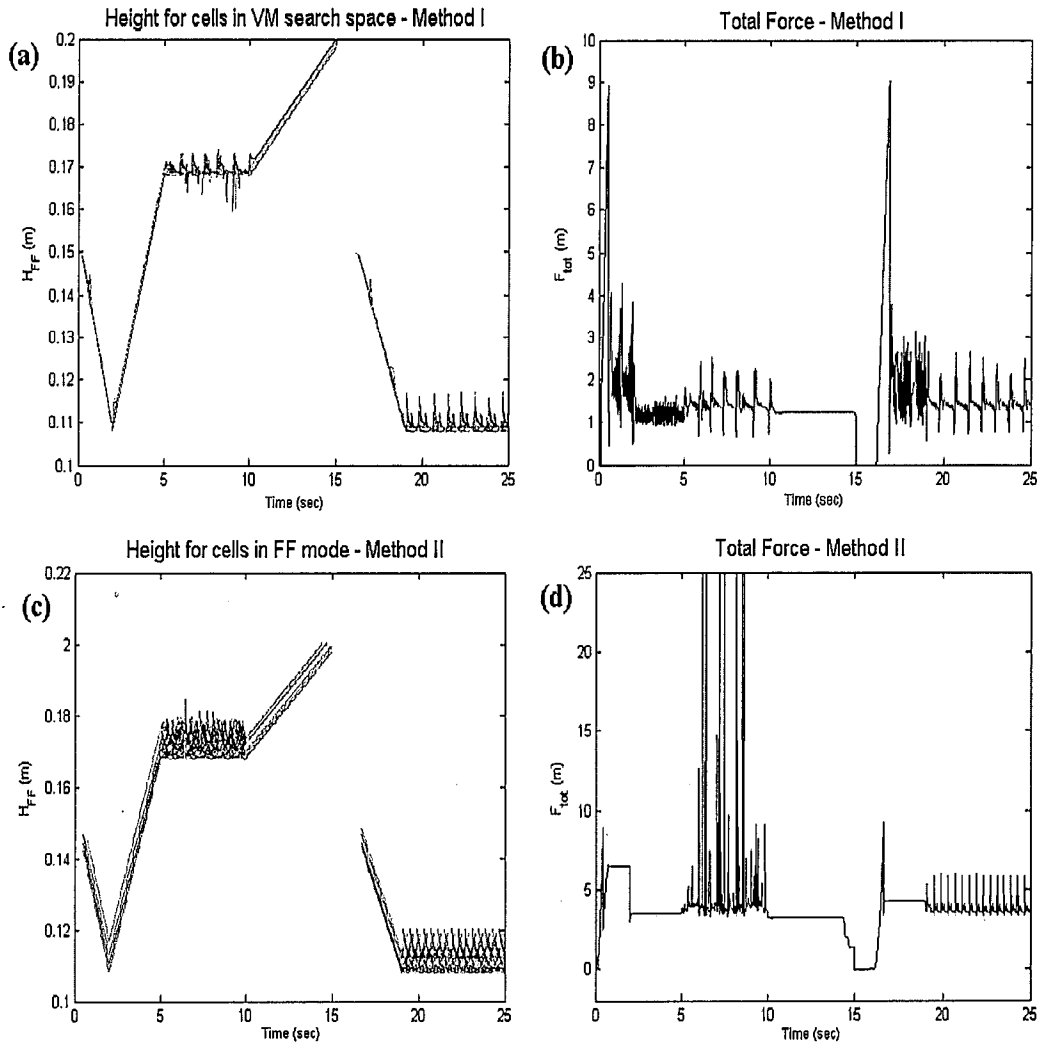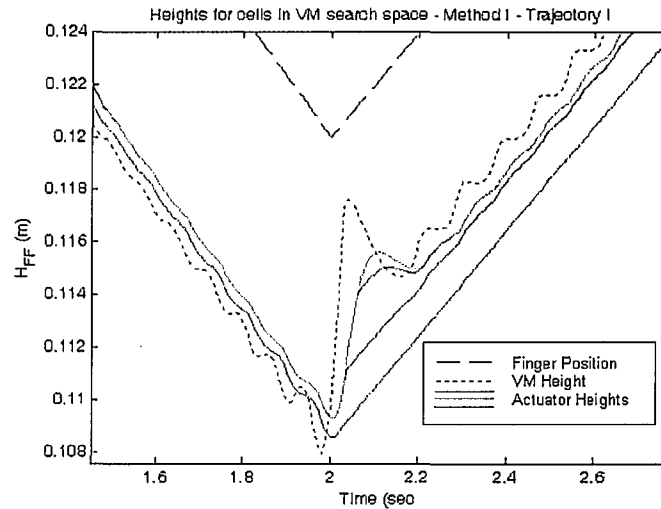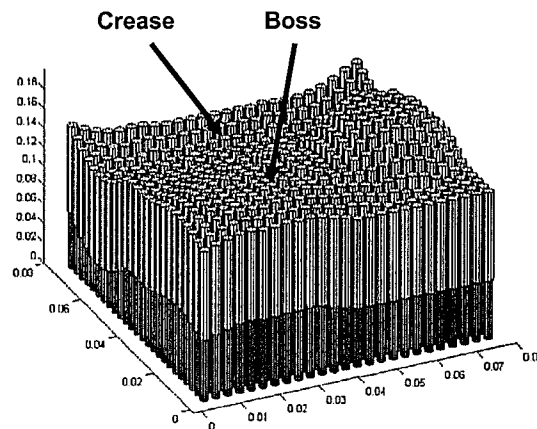

Figure 8: Selected heights and total force for both methods

Figure 9 Unwanted oscillations

Figure 10: Final surface after shaping

positions with a fully formed crease and boss.

An initial observation of Fig. 8 is that the height and force deviations when the device is tracking a horizontal finger movement (between 5s and 10s as well as 18s and 25s) are much greater for the second method. This is an expected result: the cells just outside of those under the finger are commanded to be a certain distance higher to ensure that they detect the oncoming finger, causing high forces when they are contacted. The first method, on the other hand, tracks the fingers position, and lowers the cells to anticipate the finger's arrival.

One important phenomenon is better seen by examining the detail of Fig. 8a in Fig. 9. This shows an oscillatory effect resulting from the addition of the VM model, which creates a second-order system. If simple proportional controllers are used, gains must be chosen carefully in a trade-off between minimizing oscillation and speed of response. The second method bypassed this complexity by providing direct force control of actuators in contact with

the users. This may suggest that a final Digital Clay control framework should include provision for regional height *and* force commands.

Various performance measures have been defined to help determine the importance of control parameters. For instance the root-mean-square average over time of the total force deviation (RFD) compares the total force on the finger to the force set point as defined in the last section. This quantifies how much force the user must exert over time to create a desired surface.

9 CONCLUSION

This paper has introduced a model of Digital Clay, a novel haptics device for communication of three-dimensional shape information. This model includes human interaction via a simulated fingertip. The model, though it makes a number of assumptions, has been shown to be sufficient for evaluation of coordinated control techniques. Methods for concerted shaping control have been suggested and tested within the capabilities of the simulation. The methods were validated and performance measures were used to determine correct parameter settings.

As the design of the Digital Clay device progresses, the model developed here will be updated to reflect more concrete information, and will be used to evaluate other user interaction schemes.

ACKNOWLEDGMENTS

REFERENCES

1. Rossignac, J., Allen M., Book, W., Glazer A., Ebert-Uphoff, I., et al. Finger Sculpting with Digital Clay: 3D Shape Input and Output through a Computer-Controlled Real Surface. Shape Modeling International Conference, Korea, Seoul, May 12-16, 2003.
2. Massie, T., and Salisbury, K., The PHANToM Interface: A Device for Probing Virtual Objects, ASME Winter Annual Meeting, DSC-Vol.55-1, 1994.
3. Kammermeir, P., Buss, M., and Schmidt, G. Dynamic Display of Distributed Tactile Shape Information by a Prototypical Actuator Array. IEEE/RSJ International Conference on Intelligent Robotics and Systems, 2000.
4. Wellman, P., Peine, W., Favalora, G., and Howe, R. Mechanical Design and Control of a High-Bandwidth Shape Memory Alloy Tactile Display. Proceedings of the Fifth International Symposium on Experimental Robotics. June, 1998
5. Moy, G., Wagner, C., and Fearing, R.S. A compliant tactile display for teletaction. IEEE International Conference on Robotics and Automation, San Francisco, CA, 2000.
6. Iwata, H., Yano, H., Nakaizumi, F, and Kawamura, R., Project FEELEX: Adding haptic surface to graphics. Proceedings of SIGGRAPH2001.
7. Bosscher, P. and Ebert-Uphoff, I., Digital Clay: Architecture designs for shape-generating mechanisms. IEEE International Conference on Robotics and Automation, May 2003.
8. J. A. Carretero and K. S. Breuer. Measurement and modeling of the flow characteristics of micro disc valves. Proceedings of Micro-Electro-Mechanical Systems (MEMS); ASME International Congress and Exposition, MEMS-4, 2002.

9. Fung., Y.C. Biomechanics: Mechanical properties of living tissues. Springer-Verlag, New York,1981.
10. Pawluk, D. and Howe R. Dynamic lumped response of the human fingerpad. Biomechanical Engineering, ASME, **121**, 178-183, April, 1999
11. Pawluk, D. and Howe R. Dynamic contact of the human fingerpad against a flat surface. Biomechanical Engineering, ASME, **121**, 605-610, Dec., 1999
12. Gulati, R., and Srinivasan, M. Human fingerpad under indentation I: Static and dynamic force response. Bioengineering Conference, ASME-BED, **29**, 1995.
13. Zhu, H. and Book, W. Control concepts for Digital Clay. IFAC Symposium on Robotics and Control, September, 2003.
14. Gargus, J., Kim, B., Llamas, I., Rossigniac, J., and Shaw, C. Finger Sculpting for Digital Clay., Technical Report GIT-GVU-02-22, Oct. 2002, ftp://ftp.cc.gatech.edu/pub/gvu/tr/2002/02-22.pdf.